Atmos. Chem. Phys. Discuss., 10, 17491–17525, 2010
www.atmos-chem-phys-discuss.net/10/17491/2010/
doi:10.5194/acpd-10-17491-2010

Atmospheric Chemistry and Physics Discussions

Attribution of stratospheric ozone trends to chemistry and transport: a modelling study

G. Kiesewetter, B.-M. Sinnhuber, M. Weber, and J. P. Burrows

Institute of Environmental Physics, University of Bremen, Otto-Hahn-Allee 1, 28359 Bremen, Germany

Received: 4 June 2010 – Accepted: 5 July 2010 – Published: 20 July 2010

Correspondence to: G. Kiesewetter (gregor.kiesewetter@iup.physik.uni-bremen.de)

Published by Copernicus Publications on behalf of the European Geosciences Union.

Abstract

The decrease of the concentration of ozone depleting substances (ODS) in the stratosphere over the past decade raises the question to what extent observed changes in stratospheric ozone over this period are consistent with known changes in chemical composition and possible changes in atmospheric transport. Here we present a series of ozone sensitivity calculations with a stratospheric chemistry transport model (CTM) driven with meteorological reanalyses from the European Centre for Medium Range Weather Forecast, covering the period 1978–2009. In order to account for the reversal in ODS trends, ozone trends are analysed in two periods, 1979–1999 and 2000–2009. Effects of ODS changes on the ozone chemistry are either accounted for or left out, allowing for a distinct attribution of ozone trends to the different factors of variability, namely ODS acting via gas phase chemistry, ODS acting via polar heterogeneous chemistry, and changes in transport and temperature. Modeled column ozone trends are in excellent agreement with observed trends from the Total Ozone Mapping Spectrometer (TOMS) and Solar Backscatter UV (SBUV/2) as well as the Global Ozone Monitoring Experiment (GOME/GOME2) and Scanning Imaging Absorption Spectrometer for Atmospheric Chartography (SCIAMACHY) instruments. For the 1979–1999 period we find that changes in ODS are the dominant source of the ozone trend, while changes in transport also contribute signifcantly to the overall trend. In contrast, for the period 2000–2009 the effect of ODS changes on total ozone is small. Observed ozone changes can be reproduced well with the CTM driven with meteorological reanalyses, indicating that the observed evolution of ozone over the past decade is consistent with our current understanding of chemistry and transport.

1 Introduction

Stratospheric ozone has shown large decreases during past decades, mainly attributable to the anthropogenic input of ozone depleting substances (ODS) such as

chlorofluorocarbons (CFCs) (e.g., World Meteorological Organization, 2007). The mechanisms of chemical ozone depletion have been studied extensively and are well understood, leading to the abolition of production of the responsible substances by the Montreal Protocol in 1986 and subsequent amendments and adjustments. Since the turn of the century, stratospheric concentrations of ODS have begun to decrease (World Meteorological Organization, 2007). As a result, an onset of recovery of the ozone layer is expected to be observed within the present years (Newman et al., 2006).

In order to obtain a better understanding about a possible onset of recovery, a diligent attribution of ozone trends to different contributing factors is desirable. Main actors contributing to ozone trends are changing gas phase chemistry, changing polar chemistry and its export to lower latitudes, and possible changes in stratospheric transport and temperatures. As ozone concentrations feed back on the circulation through changes in radiative heating, "chemical" and "dynamical" effects can never be fully separated (Braesicke and Pyle, 2003). Several studies have attempted to quantify dynamical and chemical influences on past ozone trends, focusing mainly on (mostly NH) mid-latitudes (Solomon et al., 1996, 1998; Hood et al., 1997; Hadjinicolaou et al., 2002; Chipperfield, 2003). Negative ozone trends from 1979 to the late 1990s have been mainly attributed to increases in stratospheric ODS loading during that period (Chipperfield, 2003). So far, only very few model studies have explicitly addressed the question of identifying ozone trend changes as a consequence of the turnaround in stratospheric chlorine loading at the end of the 20th century. Hadjinicolaou et al. (2005) analysed modeled ozone trends in two periods (1979–1993 and 1994–2003) and showed that most of the apparent recovery trend in 1994–2003 is attributable to meteorology. In a similar study, Stolarski et al. (2006) emphasized the difficulties in identifying signs of ozone recovery due to interannual variability. Several studies on observed ozone trends have shown that increases in NH total ozone since the middle 1990s were mainly driven by changes in transport and dynamics and to a lesser extent from changes in ozone depleting substances (Dhomse et al., 2006; Wohltmann et al., 2007; Harris et al., 2008).

In this study we have performed a series of sensitivity calculations with a chemistry

transport model (CTM; Sinnhuber et al., 2003) over the past 33 years (1978–2009). In the model runs, polar chemistry and gas-phase chemistry are switched between the states "constant" and "EESC-dependent". In addition, a reference run without polar chemistry was conducted. Differences in ozone amounts and trends between the different runs thus allow us to distinguish the influences of polar heterogeneous chemistry and its export, gas phase chemistry, and meteorology (through temperature or transport). Thus, our study includes most of the agents influencing ozone variability, while ignoring direct influence of the solar cycle and volcanic eruptions (indirectly, these effects are partly included through the external wind fields that drive the CTM). All analyses are performed for the "increasing stratospheric halogen loading" phase (1979–1999) and "decreasing stratospheric halogen loading" phase (2000–2009) separately. Thus, we are able to explicitly address the question of how ozone (column and profile) trends are affected by the reversal of ODS trends, and whether observed changes in stratospheric ozone over this period are consistent with known changes in chemical composition and transport.

The outline of this paper is as follows. In Sect. 2, the model and its integrations are described. Section 3 validates column ozone timeseries against satellite observations. In Sect. 4, a regression analysis of column ozone trends is presented. Trends in profile ozone are analysed in Sect. 5 and compared to trends derived from SBUV observations. Results are discussed further in Sect. 6, which attempts a more thorough decomposition of column ozone trends into contributions from different processes.

2 Model and integrations

2.1 CTM

Our stratospheric CTM (Sinnhuber et al., 2003) is run at a horizontal resolution of $3.75^{\circ} \times 2.5^{\circ}$. It uses 24 isentropic levels as vertical coordinates, ranging from 335 K to 2750 K (roughly 10–55 km). Horizontal transport is driven by analysed wind fields

and temperatures from the European Centre for Medium-Range Weather Forecast (ECMWF) – in this study, we use ERA-40 data 1979–1999 and ERA-Interim 1989–2009. Vertical transport is derived directly from interactively calculated diabatic heating rates using the MIDRAD scheme (Shine, 1987).

2.2 Gas phase chemistry

We use a time-dependent version of the linearized ozone chemistry ("Linoz v2") described by Hsu and Prather (2009), an update to the Linoz scheme introduced by McLinden et al. (2000). Although this chemistry scheme is simple, using only one ozone tracer and net production rates parametrized according to ozone volume mixing ratio (O_3), temperature (T), and ozone column above the respective grid cell (CO3), it has been shown to generate realistic ozone fields (Hsu and Prather, 2009). Dependencies of the net ozone production rate $P-L$ on the deviations of O_3, T, and CO3 from their climatological values O_{3clim}, T_{clim}, and $CO3_{clim}$ are tabled according to month, latitude and geopotential height. From O_3-O_{3clim}, $T-T_{clim}$, $CO3-CO3_{clim}$, a photochemical steady state ozone vmr (O3*ss*, equilibrium ozone vmr in the absence of transport) is calculated, against which O_3 then relaxes with a time constant $\tau=(dP-L/dO_3)^{-1}$.

In order to meet the requirements of a trend study covering more than three decades, a few adaptations to the Linoz scheme as implemented in our CTM in a previous study (Kiesewetter et al., 2010) were found useful, which are described here.

Firstly, in order to account for the changing atmospheric composition during the period of interest, we use three different Linoz tables instead of one, which were generated for stratospheric trace gas concentrations corresponding to the years 1978, 2000, and 2010 (more specifically, to tropospheric concentrations of three years earlier, in order to account for the mean stratospheric age of air). These years are chosen as the first and last years of the model integrations, and a "peak-EESC" year in between. The tables are then interpolated linearly in time to the considered day (daily interpolation avoids jumps at the turn of the year).

The temperature dependency of the Linoz chemistry scheme turned out to be prob-

lematic in the upper stratosphere, where temperature trends differ considerably between the two different meteorological datasets used, and the sensitivity of Linoz on temperature is large. A first set of runs with full T dependency showed considerable differences in upper stratospheric ozone trends depending on the met data chosen (see Sect. 5 for details). However, since this paper deals with trends, a large effect of trend uncertainties in T is undesirable and should be eliminated in order to ensure comparability between model integrations using different meteorological data. Moreover, models which account for T dependence of ozone chemistry have been shown to generate erroneous ozone trends in the upper stratosphere in a similar context (World Meteorological Organization, 2007, Chap. 3). Thus we have decided to switch off temperature dependence for the top six model levels, starting from 1044 K upwards. Effectively, this is equivalent to setting T to T_{clim} at these levels.

2.3 Polar chemistry

The effects of heterogeneous ozone destruction are included in our model in form of a simple parametrized polar chemistry as described by Kiesewetter et al. (2010). When conditions for polar stratospheric cloud (PSC) formation are met and enough sunlight is present, ozone is destroyed at a defined rate. Parameters used here are modified slightly from Kiesewetter et al. (2010): ozone lifetime (year 2000) τ=10 d and critical solar zenith angle θ=92.5°. In order to account for the changing concentrations of ODS in the stratosphere during the period of our model integrations, we scale the ozone decay rate $1/\tau$ linearly with the effective equivalent stratospheric chlorine (EESC), calculated as described by Newman et al. (2006) (age of air=5.5 yr, age spectrum width=2.75 yr, bromine scaling factor α=50). EESC was obtained from the NASA automailer system, online at http://acdb-ext.gsfc.nasa.gov/Data_services/automailer/.

A comparison of polar ozone losses in the CTM to estimates provided, e.g., in World Meteorological Organization (2007) shows that the model generally captures the variability of NH losses well, but underestimates the magnitude. Values obtained in cold winters with strong ozone depletion such as 1995/96 or 1999/2000 are around 50–

60 DU in the CTM, while the WMO assessment gives values of 80–100 DU in these years. The main reason for this behaviour lies in the construction of our polar chemistry scheme, which destroys ozone only while temperatures are cold enough for PSC formation. Thus effects of activated chlorine are missed which may occur in a denitrified vortex after PSCs themselves are no longer formed. Long-term averages of polar ozone depletion are displayed in Fig. 9 below (see Sect. 6 for details).

2.4 Model integrations

Five CTM runs were performed in total, which are labeled here according to the gas-phase chemistry (Linoz) and the polar chemistry (polarchem) scheme used. Four runs use polar chemistry; in these, Linoz and polarchem were toggled between time-dependent mode (as described above) and constant year 2000 conditions. The fifth run, which does not use polar chemistry, is used only as a reference run for diagnosing the effects of polar ozone loss.

Labels consist of two letters, the first of which corresponds to the Linoz mode and the second corresponds to polarchem mode. Letters are "*t*" for time-dependent and "*c*" for constant, and "*n*" for none (only used for polarchem). An overview of the model runs is provided in Table 1.

All model runs were performed in two parts, 1978–1999 (using ERA40 data, "E4" in the following) and 1989–2009 using ERA Interim ("EI"). A long overlap period using different meteorological analyses is desirable in order to quantify offsets in ozone concentrations due to differences in the analysed wind fields, such as discussed by e.g., Chipperfield (2003) and later in this paper. The runs starting in January 1978 are initialized from an ozone climatology (Fortuin and Kelder, 1998), while the runs starting January 1989 use output from the corresponding ERA40 driven run as initial conditions. In both cases, the first year is discarded in the analysis presented below in order to account for initial spin-up and meteorological transition.

3 Comparison to TOMS/SBUV and GOME/SCIAMACHY/GOME2 column ozone

As a first step, we have to establish that the time-dependent model run ("*tt*") represents observed ozone well. Here we show a comparison of *tt* column ozone (TO3) to observations from the TOMS/SBUV merged dataset (Stolarski and Frith, 2006), as well as the GOME/SCIAMACHY/GOME2 merged dataset ("GSG" in the following) which has been compiled from observations made by the GOME (Coldewey-Egbers et al., 2005; Weber et al., 2005), SCIAMACHY (Bovensmann et al., 1999; Bracher et al., 2005), and GOME2 (Callies et al., 2000) instruments. In the GSG merged data set the SCIAMACHY (2002-present) and GOME2 (2007-present) data have been adjusted to the GOME data record (1995-present) by determining a mean scaling factor (GOME2 and SCIAMACHY) and trend (SCIAMACHY only) in the monthly mean zonal mean ratios. Using the criterion of optimum global sampling the GSG data set is then composed of GOME1 until 2003, SCIAMACHY (2003–2006), and GOME2 after 2006. The GSG data set is described at and available from http://www.iup.uni-bremen.de/gome/wfdoas/wfdoas_merged.html (see also Weber et al., 2007).

Figure 1 shows timeseries of annual mean model TO3 (E4 and EI driven runs separately) together with TOMS/SBUV and GSG for midlatitudes and tropics. In order to enable comparison with satellite observations, the climatological ozone column below 330 K (taken from the climatology of Fortuin and Kelder, 1998) is added to modeled TO3. Modeled ozone is generally higher than the observations, with a distinct difference between the different meteorological datasets (note the shifted right-hand side axes regarding modeled TO3 during the different periods). The fact that switching meteorological analyses during a model run can lead to considerable artifacts in modeled ozone has been reported before, e.g., by Feng et al. (2007) at the transition between ERA-40 and operational analyses. In our model, mean offsets are around +20 DU (+40 DU) in NH midlatitudes, +3 DU (+4 DU) in the tropics, and +24 DU (+30 DU) in SH midlatitudes for E4 (EI) wind fields. Ozone variability is represented well especially in the 1979–1999 period (E4) and in the 2000–2009 period (EI), while the EI driven run

does not fully capture the decadal-scale increase in TO3 around the turn of the century.

The generally good agreement between model and observations is underscored by high correlation coefficients between model and observed TO3 timeseries for all months and latitudes, as shown in Fig. 2 for TOMS/SBUV in the interval 1978–1999 (CTM driven by E4 data, upper panel) and for GSG in the 1995–2009 interval (CTM driven by EI data, lower panel). For the E4 driven run, correlation coefficients are higher than 0.7 for most of the NH, higher than 0.8 in the inner tropics, and higher than 0.9 for Antarctic spring. In the case of the EI driven run, most features are similar; correlation in the inner tropics and throughout midlatitude/polar spring and summer is excellent, while the model seems to have some difficulties in reproducing subtropical (∼30°) ozone variability for single months (mainly September in the NH and March in the SH).

A significant part of the decadal-scale deviations between modeled and measured TO3 in Fig. 1 appears to be related to the 11 yr solar cycle, which is not directly accounted for in our CTM. Changes in solar activity lead to variations in column ozone in the order of 2–3% (solar maximum – solar minimum, in phase with the F10.7 flux) due to an enhancement of odd-oxygen production in the middle to upper stratosphere during high solar activity (Chipperfield, 2003). Including this influence in a similar fashion as by Chipperfield (2003) and Hadjinicolaou et al. (2005) would lower model TO3 during the mid-1990s and increase it around 1999–2003, thereby significantly reducing the differences to TOMS and GSG observations. Figure 3 shows the strong relationship of TO3 deviations in Fig. 1 (measured – modeled ozone) to the solar F10.7 flux, expressed here as the correlation coefficient in dependence of latitude and temporal displacement between ΔTO3 and F10.7. A distinct pattern of high correlation in phase with the solar cycle is visible. The signal is first observed in the tropics and then propagates to the mid-latitudes, where it appears intensified. The apparent negative timeshift of maximal correlation in the tropics (the TO3 response seems to precede the solar signal) is most probably an artifact due to the long autocorrelation timescale of the F10.7 flux. Moreover, this pattern may also in parts be influenced by the volcanic

eruptions of El Chichon (1982) and Pinatubo (1991), which both occurred during the declining phase of the solar cycle. Since our simple linear chemistry scheme does not account for stratospheric aerosol loading, the CTM misses effects caused by the influx of volcanic sulfur aerosol into the stratosphere, which contributed significantly to the strong drop in observed NH midlatitude TO3 during 1992–1993 (Sinnhuber et al., 2009).

Figure 4 illustrates the realistic variability of polar ozone in our CTM. Similar to Fig. 1, TO3 timeseries from the *tt* CTM run (corrected for TO3 below 330 K) are compared to satellite observations from the TOMS/SBUV merged ozone dataset as well as the GSG dataset. Although small offsets to satellite observations are present, polar ozone variability is captured very well in the CTM. However, trends are underestimated in both hemispheres, probably due to the choice of a linear scaling of polar chemistry with EESC.

4 Column ozone trends

In this section, we present results from a trend analysis of total column ozone from our CTM, applying a simple linear regression model. It has become common practice during recent years to use linear regression including EESC, QBO, and where appropriate volcanic and solar terms for trend analysis – the actual ozone trend is then diagnosed implicitly from the EESC fit parameter through the linear growth of the EESC curve in the 1980s (World Meteorological Organization, 2007). However, we do not apply this method here, since the time period covered includes phases of rising and falling EESC, and thus the conversion from the EESC fit parameter to ozone trend is unclear. Moreover, we cannot analyse the whole 32 yr record in one piece due to the artifacts induced in modeled ozone by the transition between the different meteorological datasets. Instead, we use a regression model that accounts only for mean ozone and a linear trend, and select time periods which do not cross the peak EESC year (in our scheme) of 2000. As noted, e.g., in the SPARC report 1 (Harris et al., 1998), neglecting the

additional terms of variability such as QBO or solar cycle does not change trend estimates as long as the analysed timespan is sufficiently longer than the timescale of variability of these terms.

Trends are analysed for two time periods, 1979–1999 (runs using E4) and 2000–2009 (runs using EI). Figure 5 shows TO3 trends relative to 1980 values for the E4 period, for all seasons. Error bars represent the 1σ uncertainty range as obtained from the standard deviation of the residua. In addition to the "full" time-dependent trend (tt), also the cc trend is shown for comparison, which represents the effects of changing circulation as well as meteorological effects acting on gas phase chemistry and polar chemistry. A detailed analysis of the differences of trends is provided in Sect. 6. TO3 trends observed in model run tt are in excellent agreement with trends in TOMS/SBUV, which confirms that the patterns of ozone variability are captured well in our CTM. Trends are generally zero near the equator (the model shows a slight negative trend around the equator that is not present in the observations) and decrease to around −0.3 to −0.5%/yr in the extratropics, except for SH high latitudes in spring when large effects of heterogeneous ozone depletion are observed (<−2%/yr in TOMS, somewhat less in tt). In this context, it is remarkable that also run cc shows a distinct downward trend in TO3 in the SH polar spring (almost 50% of the tt trend), which is a clear indication of a feedback of ozone depletion on the stratospheric circulation as discussed before by, e.g., Randel and Wu (1999). Ozone depletion causes a decrease in SH polar lower stratospheric temperatures during spring, which in turn influence the stratospheric circulation by strengthening the polar vortex and delaying its breakup, leading to decreased mixing in of ozone rich air from lower latitudes, which contributes to the decreasing trend visible in run cc. In addition, the colder vortex in turn intensifies ozone depletion during spring (e.g., Jones and Shanklin, 1995).

Figure 6 shows TO3 trends relative to 1980 values for the post peak-EESC 2000–2009 period, in comparison to trends from the GSG dataset (related to TOMS 1980 TO3, as the GSG dataset starts in 1995). In this period, trend patterns from tt and cc runs show only small differences and are both in excellent agreement to observations.

Extreme caution must be exercised when analysing trends due to the shortness of the timespan under consideration here; especially in polar regions, due to interannual variability of meteorological conditions linear trends show large uncertainties as indicated by the error bars. No significant trend is visible, except for an apparently strong negative trend in SH polar latitudes. However, a detailed investigation shows that this trend is more or less only a result of the unusually high TO3 values in 2002, caused by the early breakup of the polar vortex due to a stratospheric sudden warming (Sinnhuber et al., 2003). Varying the starting year for the trend analysis slightly (e.g., to 1998) cancels out the strong negative trend in the Antarctic, while the shape of the remaining curve remains essentially the same. Since our analysis is mainly focused on non-polar trends we decided to keep the period of analysis unchanged while referring to this issue separately. It should be noted that while absolute TO3 trends of neither tt nor cc are significant themselves, trends of their differences are, as explained in Sect. 6. Trends derived from the time-dependent run including EESC change are always above those from natural variability under chemical conditions from year 2000. The significance of trends of TO3 differences provides the opportunity to analyse the different contributions from atmospheric composition change and meteorology that contribute to them in greater detail. This is done in Sect. 6.

5 Profile trends

Figure 7 shows annual mean trends in ozone vmr for midlatitudes and tropical latitudes in the E4 period. Similar to Figs. 5 and 6, trends from the "full" time-dependent run tt are shown in comparison to SBUV observations and purely meteorological trends from run cc. SBUV observations are taken from the SBUV merged dataset (zonal 5° grid). Error bars represent 1σ uncertainty as derived from the variance of the linear regression residuals. Modeled trends are in good agreement to observed trends. General features are remarkably similar for all considered latitude bands, displaying a large downward trend in in the upper stratosphere with peak values about −0.6%/yr at

~1500 K/~42 km, a near-zero or even positive trend around 600 K/25 km, and a strong negative trend in the lower stratosphere around 380 K/16 km, which resembles the upper stratospheric trend in magnitude. This overall picture is also consistent with profile trends reported in the SPARC Report (Harris et al., 1998) which were compiled from various sources (satellite observations, sondes and ground-based instruments) for a similar period (1980–1996); especially the two negative peaks match well.

In the tropics, the pronounced decrease in modeled ozone in the lowermost stratosphere is present in the natural background run *cc* in a similar magnitude, pointing to changes in atmospheric circulation as its origin, while in the midlatitudes the influx of increasingly ozone-depleted air from polar latitudes in run *tt* contributes significantly (visible as difference between *tt* and *cc*). Due to its much less pronounced presence in the *cc* run, the strong upper stratospheric decrease in *tt* is mostly attributable to changing atmospheric composition (in particular, increasing EESC acting through the ClO_x cycle). Since T dependence of our ozone chemistry is explicitly switched off in the upper stratosphere, we cannot quantify a possible influence of T trends on observed upper stratospheric ozone trends but rather note that the trend implied by changing chemical composition and transport alone is sufficient to generate a negative ozone trend that resembles the observed trend.

The large effect of temperature trends on modeled ozone in the upper stratosphere is illustrated in Fig. 8, which shows the difference in Linoz steady state ozone (O3*ss*) evolution for the overlap interval of ERA40 and ERA Interim, when everything except the meteorological dataset is kept constant. Note that O3*ss* itself is a fictitious quantity only used in the Linoz scheme; nonetheless we show it here in order to explicitly address the difficulties caused by inconsistent T evolution in the different meteorological reanalyses. The Linoz table used in Fig. 8 is the one for 2000; modeled ozone vmr (monthly means of 1999) is used for calculation of the overhead column ozone, identical in both cases. In order to estimate the difference in O3*ss* evolution due to the different temperature data, we use a simple linear regression of temperatures at all latitudes and Theta levels to obtain a pair of "modeled" T_{E4} and T_{EI} for 1989 and

1999, for E4 and EI separately. From these, we calculate $O3ss_{E4}$ and $O3ss_{EI}$ for 1989 and 1999, differences of which are shown in Fig. 8. Considerable differences in steady state ozone evolution above $\Theta \approx 1000$ K are obvious, arising solely from different T evolution. Since ozone is close to steady state at these high altitudes, also the trend in the modeled ozone is affected in a similar magnitude. For this reason, we explicitly eliminate T dependence of the gas phase chemistry in the top six model layers in all model runs analysed in this paper by setting $T = T_{clim}$ in the Linoz chemistry calculations. As a remark, it should be noted that in spite of the different T trends, absolute T values are similar and thus also absolute ozone. Moreover, ozone above 1000 K contributes little to the total column, and thus the effect of eliminating T dependence in the uppermost levels on the TO3 trend proved negligible.

6 Contributions to total ozone trends

In this section, differences in modeled ozone trends are analysed in order to distill contributions from different processes. In particular, we seek to quantify the effects of ODS changes on TO3 evolution, acting through polar heterogeneous chemistry (and its export) as well as through gas phase chemistry, as opposed to meteorological (transport and temperature) effects. Polar heterogeneous chemistry leads to severe ozone depletion during winter and spring, after which the air mases are exported to lower latitudes. In our CTM, substantial polar ozone loss is already present before 1980, as expected from the linear scaling of the ozone destruction rate with ODS levels and the fact that EESC levels at 1980 were more than half of the peak values attained at the end of the 1990s. When comparing model runs with polar chemistry (*tt*, *tc*) to the reference run without polar chemistry (*tn*), we observe that a residual effect of polar chemistry persists at all latitudes and does not vanish throughout the year. As an example, Fig. 9 shows the magnitude of *tn*–*tc* offets during the EI period (1989–2009; numbers are somewhat smaller for E4 1979–1999). The minimal values of these offsets amount to around 2–5 DU in the northern midlatitudes (June–September), 1–2 DU in the trop-

ics, and 8–15 DU in the southern midlatitudes (March–August). Under constant ODS levels, these offsets ($tn-tc$) show considerable interannual variability related to the meteorological conditions in the preceding polar winter.

In order to separate effects of changing atmospheric composition on gas-phase chemistry and polar chemistry, we analyse differences of runs tt, ct, and cc. While tt contains full temporal evolution of gas phase and heterogeneous chemistry, cc assumes constant chemical conditions and underlies only meteorological variability. Trends of $tt-ct$ can be interpreted as the contribution of changing ODS to ozone trends through gas phase chemistry, while $ct-cc$ yields the fraction of ozone trends attributable to the effect of ODS changes on polar chemistry. Figure 10 displays these difference trends for the 1979–1999 period, along with the cc trend as zonal means for all seasons. Note that trends are given as absolute values in DU/yr here, contrary to Fig. 5 which relates them to 1980 TO3 values. The reason is the obvious ambiguity as to which reference value trends of ΔTO3 should be related to. As the cc trend itself is displayed in both Figs. 5 and 10, the reader may obtain an approximate grasp of how these absolute trends translate into relative ones. Error bars in Fig. 10 correspond to 1σ standard variation of the residuals. Since the differences $tt-ct$ and $ct-cc$ originate in information that is put into the CTM (i.e., the linear interpolation of Linoz tables and the linear scaling of the polar chemistry with EESC), it is not surprising that the residuals of a linear fit to these differences are small. For this reason, the error bars of $tt-ct$ and $ct-cc$ should be viewed with caution, as they are directly influenced by the design of our study and do not correspond to actual "uncertainty". Nevertheless, we include them here to give a feeling of how well determined the differences between the model runs are, as compared to the large variability in meteorological (cc) trends.

Given the latitudinal dependence of the "full" (tt) trend as shown in Fig. 5, changes in gas phase chemistry ($tt-ct$) make up for the main contribution to observed trends outside the polar latitudes. In all seasons except SH midlatitude summer (DJF), more than 50% of the observed trend in TO3 is explained by gas phase chemistry changes. In absolute terms, effects of ODS changes on gas phase chemistry are generally weak-

est in tropical latitudes (∼−0.2 DU/yr) and more pronounced in extratropical latitudes. Seasonality is low, resulting in an almost symmetric structure peaking during polar winter and spring (∼−0.7 DU/yr), and a slightly weaker trend in polar summer and autumn (∼−0.5 DU/yr).

On the contrary and as to be expected, influence of ODS on ozone trends due to heterogeneous chemistry and its export ($ct-cc$) shows a pronounced seasonality and latitude dependence. Polar ozone depletion is observed already during SH winter, peaking at high southern latitudes during spring (∼−1.8 DU/yr), after which the ozone depleted air masses are distributed to mid-latitudes where they cause a trend of ∼−0.35 DU/yr or ∼35% of the total observed (tt) trend during SON and DJF. Due to the warmer Arctic vortex and its earlier breakup, heterogeneous ozone depletion is generally less severe in the NH and peaks earlier in spring than in the Antarctic, resulting in a peak trend of −0.35 DU/yr during DJF and MAM at high northern latitudes. Through dispersion to lower latitudes this effect contributes around −0.15 DU/yr or ∼15% to column ozone trends in NH mid-latitude spring. Near the equator the effect of ODS through export of polar chemistry is small, as to be expected (less than −0.05 DU/yr or 10% of the total observed trend). Note that due to the large uncertainties in total (tt) trends as shown in Fig. 5, percentages of different contributions are also subject to large uncertainties although the absolute difference trends are well determined (see errorbars in Fig. 10). Alternatively to the differences presented here, one may also take $tt-tc$ (instead of $ct-cc$) as the effect of ODS changes acting through polar chemistry and its export, and conversely $tc-cc$ (instead of $tt-ct$) as the effect of ODS changes acting via gas phase chemistry. These differences show very similar trends to the ones described above, agreeing to these within less than 0.1 DU/yr (not shown in Fig. 10 to enhance readability).

Since polar column ozone loss is underestimated in our CTM (see Sect. 2.3), also the values for trends induced by ODS changes through polar chemistry presented here may be regarded as a lower boundary. The obvious slight underestimation of column ozone trends at mid-to-high latitudes as compared to satellite observations (see Fig. 5)

may serve as an indication that this is the case. However, it is not straightforward that an underestimation of the magnitude of column loss by a certain percentage should lead to an underestimation of the "ODS effect on polarchem" trend $ct-cc$ by a similar percentage, since stronger heterogeneous chemistry would increase offsets $tt-tn$ and $tc-tn$, while the $ct-cc$ trend is primarily determined by the ODS trend and the scaling factor of polarchem vs. EESC (1 in this study).

The values of trends caused by ODS changes described here compare well to results obtained by Chipperfield (2003), who reported that in a similar modelling study for the 1979–1998 period, the total effect of increasing halogen loadings (gas phase+polar chemistry) led to a reduction of midlatitude column ozone of around 20 DU in the SH and 10 DU in the NH. In our study the corresponding amounts are 16 DU in the SH and 12 DU in the NH.

The magnitude of trends caused by meteorological changes alone (cc) is comparable to those of the trends caused by changing ODS, ranging between −0.5 and +0.5 DU/yr except for polar latitudes during the ozone hole season in spring. As noted before, the strong negative trend in SH polar latitudes during SON (∼−2 DU/yr, exceeding the effect of changing ODS on polar chemistry, $ct-cc$) may clearly be interpreted as a sign of dynamical feedback of ozone depletion, as are most probably also the strong negative cc trends at high southern latitudes during DJF (∼−1 DU/yr) and high northern latitudes during MAM (∼−0.9 DU/yr). In the NH midlatitudes, meteorological changes contribute around 30–40% year-round to total ozone trends, while in the SH midlatitudes their contribution is comparably large during summer but negligible during winter months. The value of ∼35% contribution to NH midlatitude trends in spring lies between values reported by Randel et al. (2002) (20–30%) and values obtained by Hadjinicolaou et al. (2002) (more than 50%).

In addition to the decomposition of total trends into their contributions from changing ODS loading and meteorology, the latter can be further distinguished into effects of changing transport and effects of temperature trends acting on gas phase chemistry. During the last decades, stratospheric temperatures have shown a prominent

cooling trend of around −0.5 K/decade (lower stratosphere) to −2.0 K/decade (upper stratosphere), mainly attributable to increased emission of infrared radiation due to anthropogenic inputs of greenhouse gases (Shine et al., 2003). Comparison of ozone changes in the cc run to a model run with temperature dependency in Linoz switched off completely yields that in the 1979–1999 period, the influence of T changes alone contribute to a positive trend in TO3, in line with our understanding that lower temperatures favor higher ozone gas phase chemical equilibrium concentrations. Compared to the meteorological trend (cc), the ozone trend due to temperature change alone is quite small, about 0.1–0.2 DU/yr.

Figure 11 shows the trend decomposition as in Fig. 10 but for the 2000–2009 period. A distinct positive trend in column ozone is visible as an effect of ODS decreases on gas phase chemistry ($tt-ct$), while effects of a changing ozone hole chemistry ($ct-cc$) are not yet pronounced except for polar areas, where they are directly imposed by the EESC scaling. Overall, meteorological variability dominates, showing strong variations with season and latitude. As noted above, the strong negative trend in SH polar latitudes in the ozone hole season (SON) is mostly caused by the anomalous breakup of the Antarctic polar vortex in spring 2002 and vanishes when a slightly longer period of analysis is chosen.

7 Conclusions

In this paper we have attempted to quantify the contributions of changing atmospheric composition as well as temperature and circulation changes to modeled ozone trends, focusing on the non-polar latitudes. The good agreement of modeled TO3 and profile ozone trends with independent satellite observations gives us confidence that the derived diagnostics (differences of modelled TO3 trends) give a realistic representation of actual contributions. In this regard, the simplicity of our CTM using a linearized chemistry and a parameterized polar chemistry, is an advantage, as it allows for a distinct attribution of ozone changes to their processes of origin, while in a more complex

model effects of different processes are more complicated to separate.

In the period 1979–1999, we find that trends in gas phase chemistry owing to changing ODS dominated ozone evolution, contributing around 50% to NH midlatitude TO3 trends and 30–80% to SH midlatitude trends (which undergo a pronounced seasonality due to polar ozone depletion and its export in spring). As expected, effects of changing ODS through export of ozone-depleted air masses from high latitudes are strongest in SH spring, where they are responsible for ∼35% of total trends, while in the NH only ∼15% of springtime ozone trends at midlatitudes are attributable to a polar origin. In order to characterize the overall effect of export of heterogeneous chemistry to non-polar latitudes, we have to take into account a considerable offset due to polar ozone depletion which is already present in our CTM in the late 1970s. Meteorological variability, i.e. mostly changes in stratospheric circulation (including feedback from chemistry and possible influences from anthropogenic climate change), contribute up to ∼45% to midlatitude trends in the 1979–1999 period, with strong seasonality. In particular, we find a contribution of ∼35% to NH midlatitude trends in spring, in agreement with Randel et al. (2002), who derived a 20–30% contribution of circulation changes to NH midlatitude TO3 trends.

Also in the decade 2000–2009, which has seen decreasing EESC values, evolution of TO3 in our CTM is in excellent agreement to what measurements show. During this period, no significant column ozone trends are present in either of the model runs, nor in the satellite observations. Effects of decreasing ODS loading are visible after 2000 as differences between model runs; however, these effects are yet too small to enable a distinction from the expected evolution in case of constant EESC levels. Ozone evolution in this decade is overly dominated by meteorological inter-annual variability. In conlusion, we find that the evolution of the stratospheric ozone layer as observed during the last three decades is very well explained in our CTM by the combined effects of changes in gas-phase chemistry, changes in polar chemistry and its export, and meteorological variability.

Acknowledgements. We thank Juno Hsu and Michael Prather (UC Irvine) for providing the Linoz tables used in this study and sharing their expertise with us. We thank NASA GSFC (TOMS Science Team) for providing the TOMS and SBUV data (Merged Ozone Dataset) used in this study. ECMWF ERA-40 and ERA Interim data used in this study have been obtained from the ECMWF Data Server through the special project DECDIO. Parts of this work have been funded by the German Research Foundation (DFG) under the priority programme "CAWSES – Climate and Weather of the Sun Earth System". Work related to merging the GOME, SCIAMACHY, and GOME2 total ozone record has been funded in parts by the BMBWi Project ENVIVAL-LIFE and DFG Research Unit "Stratospheric Change and its Role for Climate Prediction" (SHARP).

References

Bovensmann, H., Burrows, J. P., Buchwitz, M., Frerick, J., Noel, S., Rozanov, V. V., Chance, K. V., and Goede, A. P. H.: SCIAMACHY: mission objectives and measurement modes, J. Atmos. Sci., 56, 127–150, 1999. 17498

Bracher, A., Lamsal, L. N., Weber, M., Bramstedt, K., Coldewey-Egbers, M., and Burrows, J. P.: Global satellite validation of SCIAMACHY O_3 columns with GOME WFDOAS, Atmos. Chem. Phys., 5, 2357–2368, doi:10.5194/acp-5-2357-2005, 2005. 17498

Braesicke, P. and Pyle, J. A.: Changing ozone and changing circulation in northern midlatitudes: possible feedbacks?, Geophys. Res. Lett., 30, 1059, doi:10.1029/2002GL015973, 2003. 17493

Callies, J., Corpaccioli, E., Eisinger, M., Hahne, A., and Lefebvre, A.: GOME-2 – METOP's second-generation sensor for operational ozone monitoring, ESA Bull.-Eur. Space, 102, 28–36, 2000. 17498

Chipperfield, M. P.: A three-dimensional model study of long-term mid-high latitude lower stratosphere ozone changes, Atmos. Chem. Phys., 3, 1253–1265, doi:10.5194/acp-3-1253-2003, 2003. 17493, 17497, 17499, 17507

Coldewey-Egbers, M., Weber, M., Lamsal, L. N., de Beek, R., Buchwitz, M., and Burrows, J. P.: Total ozone retrieval from GOME UV spectral data using the weighting function DOAS approach, Atmos. Chem. Phys., 5, 1015–1025, doi:10.5194/acp-5-1015-2005, 2005. 17498

Dhomse, S., Weber, M., Wohltmann, I., Rex, M., and Burrows, J. P.: On the possible causes

of recent increases in northern hemispheric total ozone from a statistical analysis of satellite data from 1979 to 2003, Atmos. Chem. Phys., 6, 1165–1180, doi:10.5194/acp-6-1165-2006, 2006. 17493

Feng, W., Chipperfield, M. P., Dorf, M., Pfeilsticker, K., and Ricaud, P.: Mid-latitude ozone changes: studies with a 3-D CTM forced by ERA-40 analyses, Atmos. Chem. Phys., 7, 2357–2369, doi:10.5194/acp-7-2357-2007, 2007. 17498

Fortuin, J. F. P. and Kelder, H.: An ozone climatology based on ozonesondes and satellite measurements, J. Geophys. Res., 103, 31709–31734, 1998. 17497, 17498

Hadjinicolaou, P., Jrrar, A., Pyle, J. A., and Bishop, L.: The dynamically driven long-term trend in stratospheric ozone over northern middle latitudes, Q. J. Roy. Meteor. Soc., 128, 1393–1412, 2002. 17493, 17507

Hadjinicolaou, P., Pyle, J. A., and Harris, N. R. P.: The recent turnaround in stratospheric ozone over northern middle latitudes: a dynamical modeling perspective, Geophys. Res. Lett., 32, 12821, doi:10.1029/2005GL022476, 2005. 17493, 17499

Harris, N. R. P., Hudson, R., and Phillips, C. (Eds.): Assessment of trends in the vertical distribution of ozone. SPARC Rep. 1, WMO-Ozone Research and Monitoring Project Rep. 43, 1998. 17500, 17503

Harris, N. R. P., Kyrö, E., Staehelin, J., Brunner, D., Andersen, S.-B., Godin-Beekmann, S., Dhomse, S., Hadjinicolaou, P., Hansen, G., Isaksen, I., Jrrar, A., Karpetchko, A., Kivi, R., Knudsen, B., Krizan, P., Lastovicka, J., Maeder, J., Orsolini, Y., Pyle, J. A., Rex, M., Vanicek, K., Weber, M., Wohltmann, I., Zanis, P., and Zerefos, C.: Ozone trends at northern mid- and high latitudes – a European perspective, Ann. Geophys., 26, 1207–1220, doi:10.5194/angeo-26-1207-2008, 2008. 17493

Hood, L. L., McCormack, J. P., and Labitzke, K.: An investigation of dynamical contributions to midlatitude ozone trends in winter, J. Geophys. Res., 102, 13079–13093, 1997. 17493

Hsu, J. and Prather, M. J.: Stratospheric variability and tropospheric ozone, J. Geophys. Res., 114, D06102, doi:10.1029/2008JD010942, 2009. 17495

Jones, A. E. and Shanklin, J. D.: Continued decline of total ozone over Halley, Antarctica, since 1985, Nature, 376, 409–411, 1995. 17501

Kiesewetter, G., Sinnhuber, B.-M., Vountas, M., Weber, M., and Burrows, J. P.: A long-term stratospheric ozone dataset from assimilation of satellite observations: high-latitude ozone anomalies, J. Geophys. Res., 115, D10307, doi:10.1029/2009JD013362, 2010. 17495, 17496

McLinden, C. A., Olsen, S. C., Hannegan, B., Wild, O., Prather, M. J., and Sundet, J.: Stratospheric ozone in 3-D models: a simple chemistry and the cross-tropopause flux, J. Geophys. Res., 105, 14653–14665, 2000. 17495

Newman, P. A., Nash, E. R., Kawa, S. R., Montzka, S. A., and Schauffler, S. M.: When will the Antarctic ozone hole recover?, Geophys. Res. Lett., 33, L12814, doi:10.1029/2005GL025232, 2006. 17493, 17496

Randel, W. J. and Wu, F.: Cooling of the arctic and antarctic polar stratospheres due to ozone depletion, J. Climate, 12, 1467–1469, 1999. 17501

Randel, W. J., Wu, F., and Stolarski, R.: Changes in column ozone correlated with the stratospheric EP flux, J. Meteorol. Soc. Jpn., 80, 849–862, 2002. 17507, 17509

Shine, K. P.: The middle atmosphere in the absence of dynamical heat fluxes, Q. J. Roy. Meteor. Soc., 113, 603–633, 1987. 17495

Shine, K. P., Bourqui, M. S., de F. Forster, P. M., Hare, S. H. E., Langematz, U., Braesicke, P., Grewe, V., Ponater, M., Schnadt, C., Smith, C. A., Haigh, J. D., Austin, J., Butchart, N., Shindell, D. T., Randel, W. J., Nagashima, T., Portmann, R. W., Solomon, S., Seidel, D. J., Lanzante, J., Klein, S., Ramaswamy, V., and Schwarzkopf, M. D.: A comparison of model-simulated trends in stratospheric temperatures, Q. J. Roy. Meteor. Soc., 129, 1565–1588, doi:10.1256/qj.02.186, 2003. 17508

Sinnhuber, B.-M., Weber, M., Amankwah, A., and Burrows, J. P.: Total ozone during the unusual Antarctic winter of 2002, Geophys. Res. Lett., 30, 1580, doi:10.1029/2002GL016798, 2003. 17494, 17502

Sinnhuber, B.-M., Sheode, N., Sinnhuber, M., Chipperfield, M. P., and Feng, W.: The contribution of anthropogenic bromine emissions to past stratospheric ozone trends: a modelling study, Atmos. Chem. Phys., 9, 2863–2871, doi:10.5194/acp-9-2863-2009, 2009. 17500

Solomon, S., Portmann, R. W., Garcia, R., Thomason, L. W., Poole, L. R., and McCormick, M.: The role of aerosol variations in anthropogenic ozone depletion at northern midlatitudes, J. Geophys. Res., 101, 6713–6727, 1996. 17493

Solomon, S., Portmann, R. W., Garcia, R. R., Randel, W., Wu, F., Nagatani, R., Gleason, J., Thomason, L., Poole, L. R., and Mc-Cormick, M. P.: Ozone depletion at mid-latitudes: coupling of volcanic aerosols and temperature variability to anthropogenic chlorine, Geophys. Res. Lett., 28, 1871–1874, 1998. 17493

Stolarski, R. S. and Frith, S. M.: Search for evidence of trend slow-down in the long-term TOMS/SBUV total ozone data record: the importance of instrument drift uncertainty, Atmos.

Chem. Phys., 6, 4057–4065, doi:10.5194/acp-6-4057-2006, 2006. 17498
Stolarski, R. S., Douglass, A. R., Steenrood, S., and Pawson, S.: Trends in stratospheric ozone: lessons learned from a 3-D chemical transport model, J. Atmos. Sci., 63, 1028–1041, 2006. 17493
Weber, M., Lamsal, L. N., Coldewey-Egbers, M., Bramstedt, K., and Burrows, J. P.: Pole-to-pole validation of GOME WFDOAS total ozone with groundbased data, Atmos. Chem. Phys., 5, 1341–1355, doi:10.5194/acp-5-1341-2005, 2005. 17498
Weber, M., Lamsal, L. N., and Burrows, J. P.: Improved SCIAMACHY WFDOAS total ozone retrieval: Steps towards homogenising long-term total ozone datasets from GOME, SCIAMACHY, and GOME2, in: Proc. "Envisat Symposium 2007", Montreux, Switzerland, 23–27 April 2007, ESA SP-636, 2007. 17498
Wohltmann, I., Lehmann, R., Rex, M., Brunner, D., and Mader, J.: A process-oriented regression model for column ozone, J. Geophys. Res., 112, D12304, doi:10.1029/2006JD007573, 2007. 17493
World Meteorological Organization: Scientific Assessment of of Ozone Depletion: 2006, Global Ozone Research and Monitoring Project – Report No. 50, 2007. 17493, 17496, 17500

Table 1. Model runs analysed in this paper, distinguished by the gas phase chemistry (Linoz) mode and polar chemistry (polarchem) mode used. For details see text.

Run	Linoz	polarchem
tt	time-dependent	∝EESC
ct	const ODS levels (2000)	∝EESC
tc	time-dependent	const ODS levels (2000)
cc	const ODS levels (2000)	const ODS levels (2000)
tn	time-dependent	off

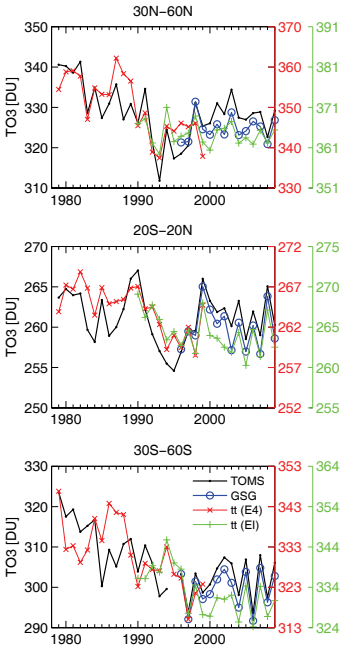

Fig. 1. Total ozone (TO3) annual means from the *tt* (time-dependent chemistry) model run, as compared to the TOMS/SBUV merged TO3 dataset ("TOMS") and the GOME/SCIAMACHY/GOME2 merged datasets ("GSG"). Model runs are performed in two periods, 1979–1999 using ERA40 data (red ×), and 1990–2009 using ERA Interim (green +). Modeled TO3 shows different offsets to satellite observations during the two periods, which are accounted for by the shifted right-hand axes (middle axis 1979–1999, far right axis 1990–2009). The climatological ozone column below 330 K has been added to modeled TO3.

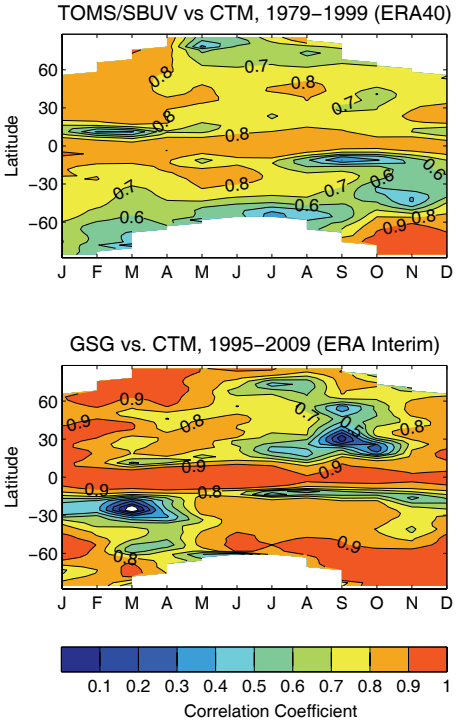

Fig. 2. Correlation between observed and modeled TO3 (*tt*) monthly mean timeseries: TOMS/SBUV vs. CTM in the period 1979–1999 (upper panel, model driven by ERA40) and GOME/SCIAMACHY/GOME2 vs. CTM in the period 1990–2009 (lower panel, model driven by ERA Interim).

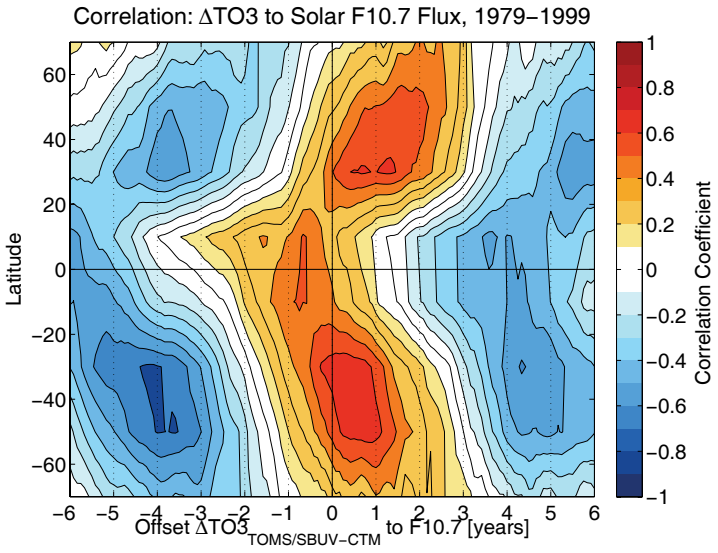

Fig. 3. Correlation between TO3 deviation (TOMS/SBUV observations – CTM) to the Solar F10.7 radio flux, with respect to latitude and temporal offset (=delay in TO3 response). For better comparison, the TO3 offset has been deseasonalized.

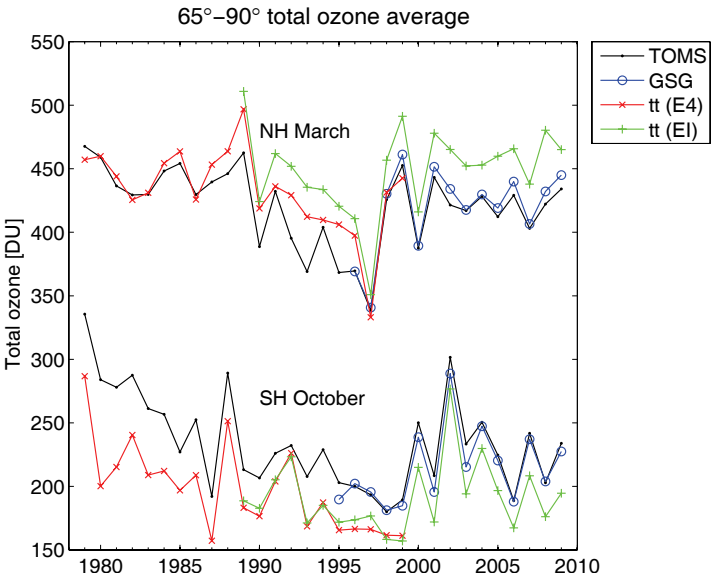

Fig. 4. Springtime polar TO3 from the *tt* (time-dependent chemistry) model run, as compared to the TOMS/SBUV merged TO3 dataset ("TOMS") and the GOME/SCIAMACHY/GOME2 merged datasets ("GSG"). Model runs are performed in two periods, 1979–1999 using ERA40 wind fields (red ×), and 1990–2009 using ERA Interim (green +). The climatological ozone column below 330 K has been added to modeled TO3.

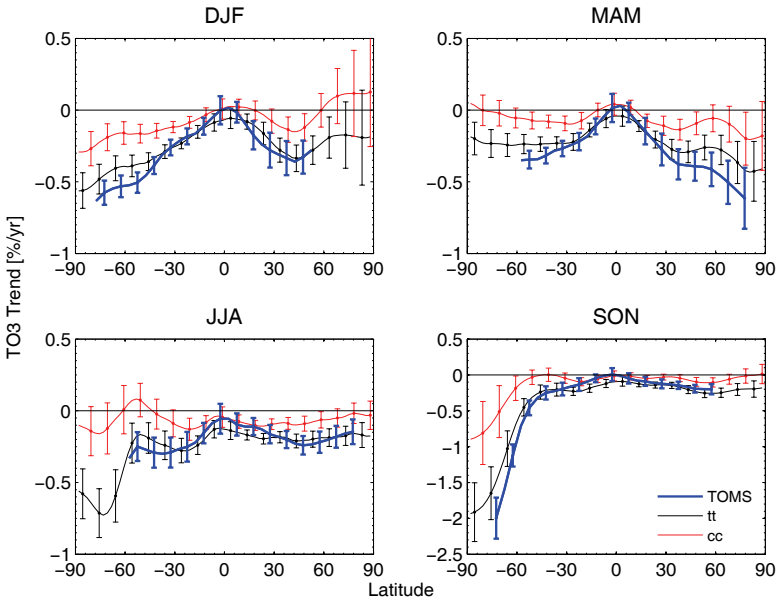

Fig. 5. Modeled TO3 trends as compared to TOMS/SBUV TO3 trends, in the period 1979–1999. Trends from model runs with time-dependent chemistry and polar chemistry (*tt*, black line with dots) and constant conditions (*cc*, red line with dots) are shown. Trends are given in percent of 1980 values per year. Error bars represent the 1σ variance as obtained from the residuals of the linear fit.

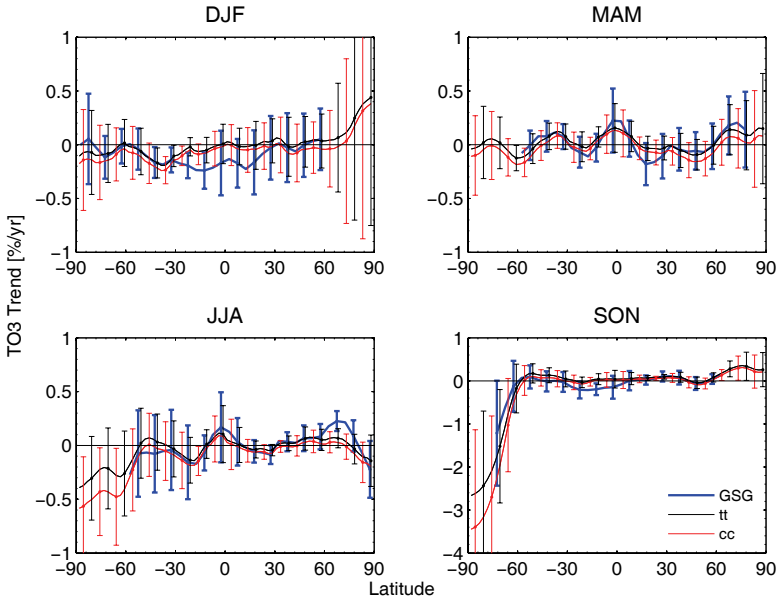

Fig. 6. Modeled TO3 trends as compared to GOME/SCIAMACHY/GOME2 ("GSG") TO3 trends, in the period 2000–2009. Trends from model runs with time-dependent chemistry and polar chemistry (*tt*, black line with dots) and constant conditions (*cc*, red line with dots) are shown. Trends are given in percent of 1980 values per year (GSG is related to TOMS 1980 values). Error bars represent the 1σ variance as obtained from the residuals of the linear fit.

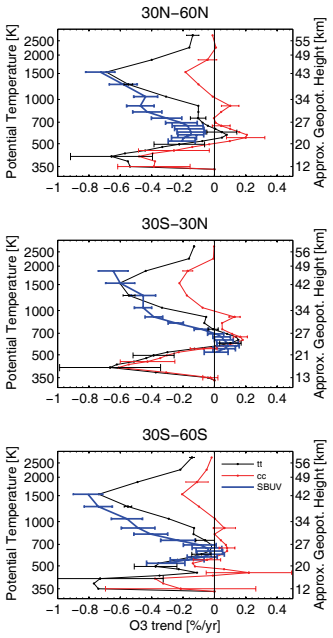

Fig. 7. Modeled O_3 trends as compared to SBUV O_3 trends, in the period 1979–1999. Trends from model runs with time-dependent chemistry and polar chemistry (*tt*, black line with dots) and constant conditions (*cc*, red line with dots) are shown. Trends are given in percent of 1980 values per year. Error bars represent the 1σ variance as obtained from the residuals of the linear fit.

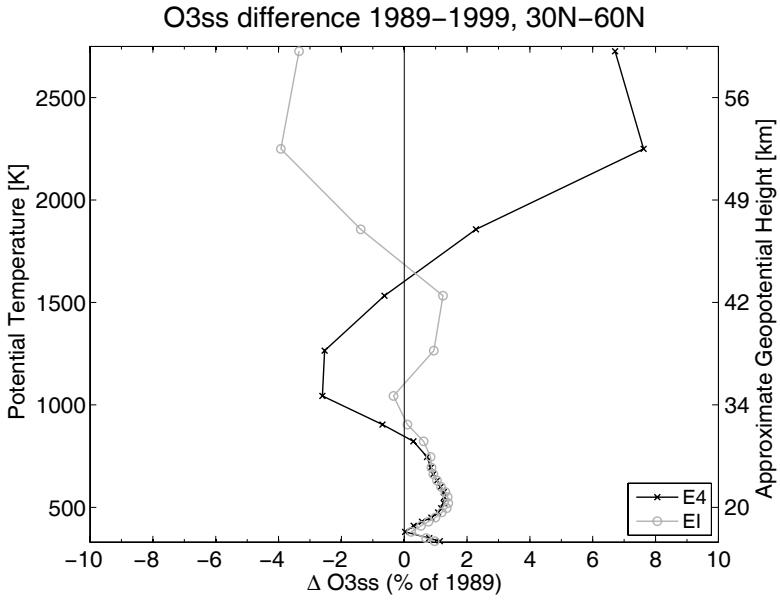

Fig. 8. Sensitivity of Linoz steady state ozone to temperature trends in the overlap period of ERA40 and ERA Interim reanalyses. Annual mean trends for 1989–1999, 30 N–60 N, calculated as O3*ss* (T(1999)) – O3*ss* (T(1989)), with all other factors kept constant (i.e., Linoz chemical table, overhead column ozone). Large differences in the upper stratosphere are obvious as a result of different T trends in the two datasets.

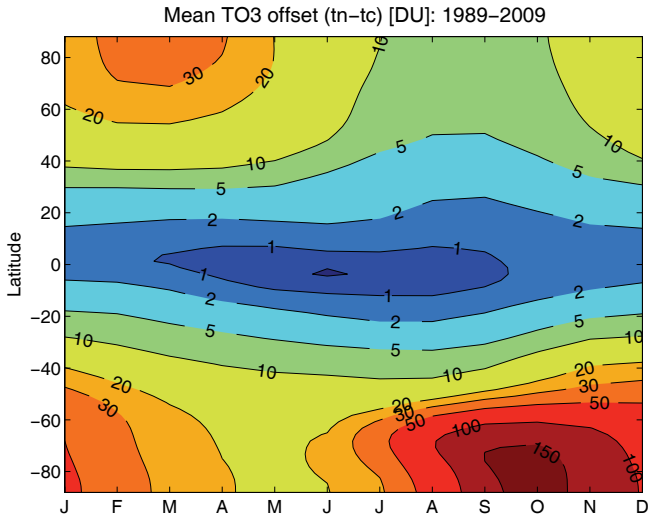

Fig. 9. TO3 offsets due to polar ozone depletion and its export (differences of runs $tn-tc$), given in DU for all latitudes and months, averaged over the ERA Interim driven period (1989–2009).

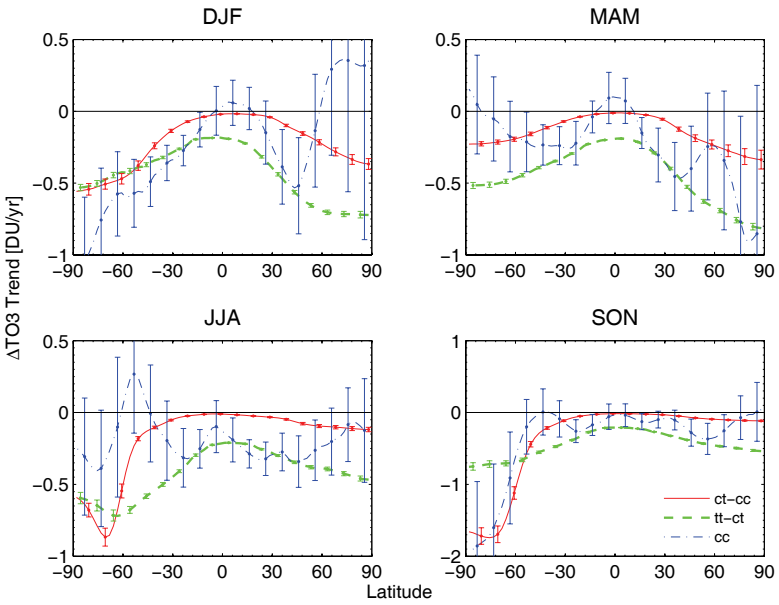

Fig. 10. Attribution of TO3 trends in the 1979–1999 period to effects of ODS change on gas phase chemistry ($tt-ct$), ODS change on polar chemistry ($ct-cc$), and natural variability under constant atmospheric composition (cc).

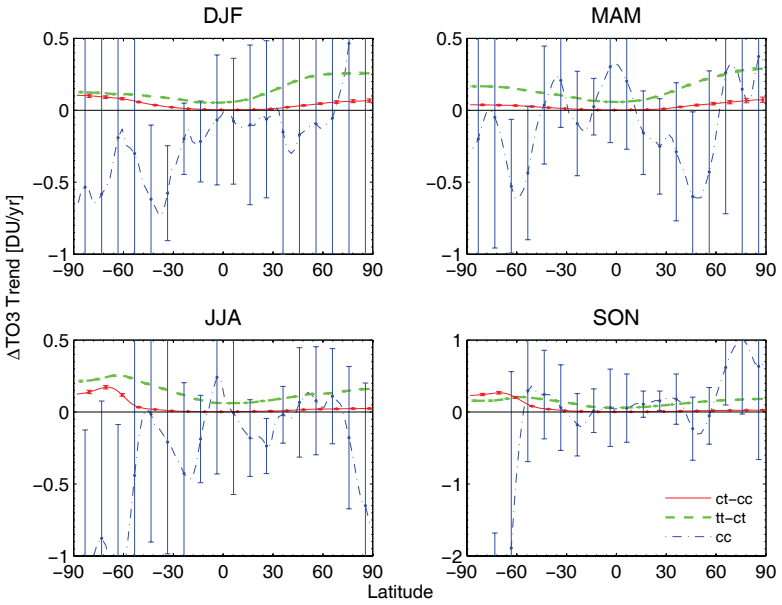

Fig. 11. As Fig. 10, but for the 2000–2009 period. Attribution of TO3 trends to effects of ODS change on gas phase chemistry ($tt-ct$), ODS change on polar chemistry ($ct-cc$), and natural variability under constant atmospheric composition (cc).